QUARTERLY JOURNAL OF THE ROYAL METEOROLOGICAL SOCIETY
Q. J. R. Meteorol. Soc. **135**: 53–66 (2009)
Published online 9 December 2008 in Wiley InterScience
(www.interscience.wiley.com) DOI: 10.1002/qj.350

Modelling of chemical and physical aerosol properties during the ADRIEX aerosol campaign

G. Myhre,[a,b]* T. F. Berglen,[a] C. R. Hoyle,[a] S.A. Christopher,[c] H. Coe,[d] J. Crosier,[d] P. Formenti,[e] J.M. Haywood,[f†] M. Johnsrud,[g] T.A. Jones,[c] N. Loeb,[h‡] S. Osborne[f†] and L.A. Remer[i‡]

[a]*University of Oslo, Department of Geosciences, Norway*
[b]*Centre for International Climate and Environmental Research – Oslo, Norway*
[c]*Dept. of Atmospheric Science, The University of Alabama in Huntsville, Huntsville, Alabama, USA*
[d]*University of Manchester, UK*
[e]*LISA, Universités Paris 12 et Paris 7, Créteil, France*
[f]*Met Office, Exeter, UK*
[g]*Norwegian Institute for Air Research (NILU), Norway*
[h]*NASA Langley Atmospheric Research Center (LaRC), Hampton, Virginia, USA*
[i]*Laboratory for Atmospheres, NASA Goddard Space Flight Center (GSFC), Greenbelt, Maryland, USA*

ABSTRACT: A global aerosol model with relatively high resolution is used to simulate the distribution and radiative effect of aerosols during the Aerosol Direct Radiative Impact Experiment (ADRIEX) campaign in August and September 2004. The global chemical transport model Oslo CTM2 includes detailed chemistry, which is coupled to aerosol partitioning of sulphate, nitrate and secondary organic aerosols. In accordance with aircraft observations the aerosol model simulates a dominance of secondary aerosols compared to primary aerosols in the ADRIEX study region. The model underestimates the aerosol optical depth (AOD) at 550 nm in the main region of the campaign around Venice. This underestimation mainly occurs during a 3–4 day period of highest AODs. At two AERONET (Aerosol Robotic Network) stations related to the ADRIEX campaign outside the Po valley area, the model compares very well with the observed AOD. Comparisons with observed chemical composition show that the model mainly underestimates organic carbon, with better agreement for other aerosol species. The model simulations indicate that the emission of aerosols and their precursors may be underestimated in the Po valley. Recent results show a large spread in radiative forcing due to the direct aerosol effect in global aerosol models, which is likely linked to large differences in the vertical profile of aerosols and aerosol absorption. The modelled vertical profile of aerosol compares reasonably well to the aircraft measurements as was the case in two earlier campaigns involving biomass burning and dust aerosols. The radiative effect of aerosols over the northern part of the Adriatic Sea agrees well with the mean of three satellite-derived estimates despite large differences between the satellite-derived data. The difference between the model and the mean of the satellite data is within 10% for the radiative effect. The radiative forcing due to anthropogenic aerosols is simulated to be negative in the ADRIEX region with values between −5 and −2 W m^{-2}. Copyright © 2008 Royal Meteorological Society and Crown Copyright

KEY WORDS aircraft measurements; secondary organic aerosols; radiative forcing

Received 27 February 2008; Revised 9 September 2008; Accepted 27 October 2008

1. Introduction

Substantial progress has been made on improving the understanding and knowledge of aerosols and their climate impact. However, global estimates of the total direct aerosol effect differ substantially and even the sign may differ in some estimates (Bellouin *et al.*, 2005; Schulz *et al.*, 2006). Large differences can also be found between estimates of the direct aerosol effect for the various aerosol compounds (Schulz *et al.*, 2006). Modelling (Kinne *et al.*, 2006; Textor *et al.*, 2006), aerosol satellite retrievals (Kaufman *et al.*, 2002; Remer *et al.*, 2005) and aerosol campaigns (Novakov *et al.*, 1997; Bates *et al.*, 1998; Raes *et al.*, 2000; Ramanathan *et al.*, 2001; Swap *et al.*, 2003; Tanré *et al.*, 2003; Kahn *et al.*, 2004) have all contributed to better understanding of the aerosols, their distributions and climate effect. Many aerosol campaigns around the world have taken place, e.g. TARFOX, ACE1, ACE2, ACE-ASIA, SAFARI-2000, INDOEX, SHADE, and MINOS, resulting in much improved knowledge on aerosol composition, aerosol optical properties, and radiative effect (Satheesh and Ramanathan, 2000; Lelieveld *et al.*, 2001, 2002; Haywood *et al.*, 2003; Quinn and Bates, 2005). Over industrialized regions of Europe the

*Correspondence to: G. Myhre, Department of Geosciences, University of Oslo, PO Box 1022 Blindern, 0315 Oslo, Norway.
E-mail: gunnar.myhre@geo.uio.no
†The contributions of J.M. Haywood and S. Osborne were written in the course of their employment at the Met Office, UK and are published with the permission of the Controller of HMSO and the Queen's Printer for Scotland.
‡The contributions of N. Loeb and L.A. Remer were prepared as part of their official duties as United States Federal Government employees.

aerosol chemical composition is observed to be quite complex (Putaud *et al.*, 2004) and the radiative effect of the aerosols in this region is uncertain.

The Aerosol Direct Radiative Impact Experiment (ADRIEX) (Highwood *et al.*, 2007) took place in August and September 2004 over the Adriatic Sea and Po Valley, and was based in Treviso, Italy. The main goal of the campaign was to characterize the aerosol composition, radiative properties, vertical profile, and the radiative impact of industrial aerosols in the Adriatic Sea and Black Sea regions (Highwood *et al.*, 2007). Few previous aerosol campaigns have investigated industrial pollution from Europe. Measurements of aerosol chemical composition and optical properties conducted onboard the UK community BAe 146 aircraft of the Facility for Airborne Atmospheric Measurements (FAAM) were a central part of the campaign. Also, ground-based measurements with sun-photometers and lidars were included, and aircraft measurements were co-ordinated with overpasses from satellites that provide aerosol remote sensing. This paper describes an aerosol modelling activity related to the ADRIEX campaign.

In this study, the global aerosol transport model Oslo CTM2 is used to calculate the radiative effect of the aerosols over the ADRIEX region. This model has been used to calculate the radiative effect of aerosol in two earlier campaigns, SAFARI-2000 (Myhre *et al.*, 2003a) and SHADE (Myhre *et al.*, 2003b), giving good agreement with aircraft measurements. The model results also correspond well with satellite-derived aerosol optical depth (AOD) and radiative effect, as well as Aerosol Robotic Network (AERONET) data (Myhre *et al.*, 2007). A comparison with the available measurements will be shown for both the chemical composition and optical properties of the aerosol. Section 2 gives a brief description of the model. Section 3 presents a comparison of modelled and measured chemical composition and vertical profiles. The model AOD is compared both with sun-photometers and aerosol satellite retrievals. This section also includes model simulations of the radiative effect of the aerosols and comparison with satellite data to enable better quantification of the radiative forcing due to the aerosols' direct effect. Conclusions are drawn in section 4.

2. Models and methods

The Oslo CTM2 is an off-line global chemistry and aerosol transport model. In this study, the Oslo CTM2 model uses the European Centre for Medium-Range Weather Forecasts Integrated Forecast System (ECMWF IFS) meteorological data for the campaign period as well as 3 months of meteorological data prior to the campaign period to provide model spin-up. Global high-resolution data on a 1×1 degree horizontal grid and 40 vertical layers are adopted and a time resolution of 3 h is used.

The model includes the major aerosol components: mineral dust, sea salt, sulphate, black carbon (BC) and organic carbon (OC) from fossil fuel and biomass burning (Myhre *et al.*, 2007), and nitrates (Myhre *et al.*, 2006). A module for the treatment of secondary organic carbon aerosol (SOA) has recently been implemented (Hoyle *et al.*, 2007). The model has been compared to a large number of aerosol observations (Myhre *et al.*, 2008).

Mineral dust is described in Grini *et al.* (2005) and the emissions are calculated based on model wind speed and vegetation type. Likewise the emissions of sea salt (Grini *et al.*, 2002) are wind driven. The oxidation of SO_2 to sulphate (Berglen *et al.*, 2004) is calculated on-line with the tropospheric oxidants, i.e. OH in the gas phase and O_3, HO, HONO and metals in the aqueous phase. Global emissions of anthropogenic SO_2 for the year 2000 are taken from Dentener *et al.* (2006) although for Europe these emission data are augmented by the Co-operative Programme for Monitoring and Evaluation of the Long-range Transmission of Air Pollutants in Europe (EMEP) emissions for 2004 (Vestreng *et al.*, 2007).

The conversion rate of the carbonaceous aerosols from hydrophobic to hydrophilic has been suggested to be substantially longer (Maria *et al.*, 2004) than usually applied in global aerosol models. We have adopted the conversion rates given in Maria *et al.* (2004) for primary carbonaceous aerosols (i.e. those emitted directly to the atmosphere) giving a conversion rate from hydrophobic to hydrophilic of 24% per day for BC and 21% per day for OC. Fossil-fuel primary carbonaceous particle emission data are from Bond *et al.* (2004), and emissions of carbonaceous particles from biomass burning are from the Global Fire Emission Database (GFED) for the year 2004 (van der Werf *et al.*, 2006). BC emissions are assumed to be 80% hydrophobic and 20% hydrophilic, while OC emissions are assumed to be 50% hydrophobic and 50% hydrophilic. An organic mass to OC (OM/OC) ratio of 1.6 is adopted in the simulations based on Turpin and Lim (2001) and Polidori *et al.* (2008).

Emissions of volatile organic carbon from both biogenic and anthropogenic sources are oxidised by reaction with either OH, O_3 or NO_3, and the partitioning of the resulting semi-volatile products to existing organic aerosol, and ammonium sulphate aerosol, is calculated based on the two-product model of Odum *et al.* (1996). Comparisons with observations showed that allowing SOA to partition to sulphate aerosols in addition to organic aerosols resulted in improved agreement compared to when only partitioning to organic aerosols was allowed (Hoyle *et al.*, 2007). The gas phase chemistry scheme (O_3-NO_x-volatile organic compounds (VOC)) is described in Berntsen and Isaksen (1997) and includes 51 components. Emissions of tropospheric gases are those developed for the Precursors of Ozone and their Effect on the Troposphere project (POET: Olivier *et al.*, 2003).

Nitrate is implemented in the Oslo CTM2 using the Equilibrium Simplified Aerosol Module (EQSAM: Metzger *et al.*, 2002b). In the Oslo CTM2, nitrate can be formed as fine mode ammonium nitrate or on existing sea salt particles that mostly are coarse mode (Myhre *et al.*, 2006). The treatment of nitrate has been modified compared to the standard EQSAM module (Metzger *et al.*, 2002a). For this study we have changed the

DOI: 10.1002/qj

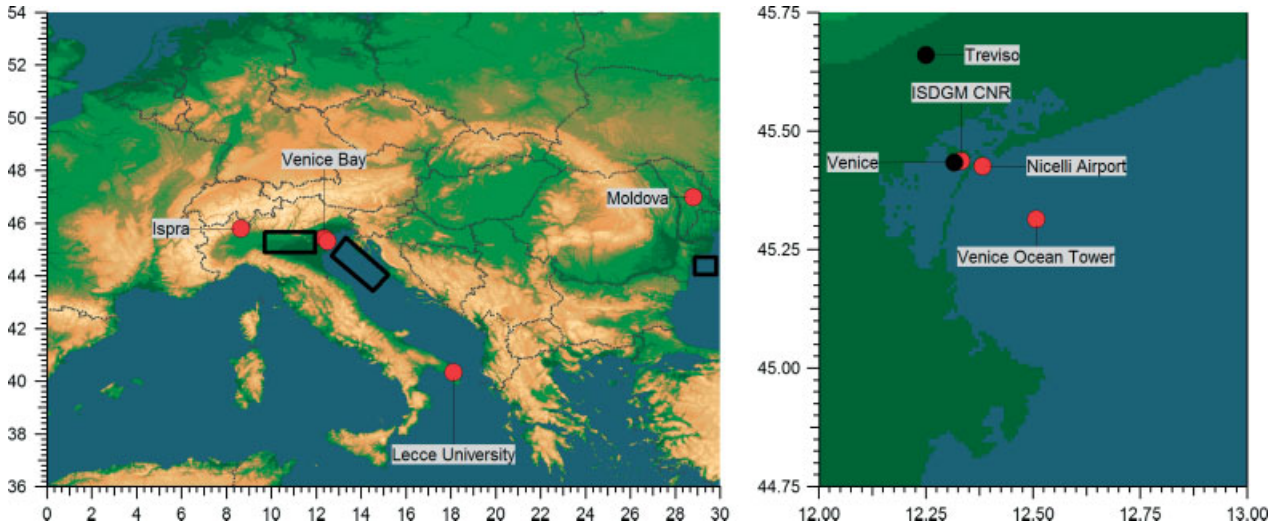

Figure 1. Map of the ADRIEX region with location of aircraft measurements and AERONET stations.

equilibrium constant K_{eq} for the NH_4NO_3 (s) $\leftrightarrow NH_3$ (g) $+HNO_3$ (g) equilibrium. The value $K_{eq} = 57.46$ ppb^2 is normally applied in this scheme. In the literature the reported values range from 30 to 59 ppb^2 (see Ansari and Pandis (1999) and references therein). Here we have used the $K_{eq} = 30$ ppb^2 giving more NH_4NO_3. Emissions of NH_3 are those from Bouwman *et al.* (1997).

The size distribution is explicitly modelled in the Oslo CTM2 for mineral dust and sea salt particles(Grini *et al.*, 2002, 2005), whereas for the other aerosol components predefined size distributions based on observations are applied (Myhre *et al.*, 2007). Osborne *et al.* (2007) show that the aerosol size distribution from ADRIEX is very similar to the size distribution from other campaigns with industrial pollution. The radiative forcing is shown to be rather robust (variation of about 10%) to the size distribution as long as accumulation mode particles dominate (Myhre *et al.*, 2004). Optical properties based on Mie theory and radiative transfer calculations are calculated as in Myhre *et al.* (2007). External mixture of the aerosols is assumed. The simulated aerosols have no impact on the cloud formation or the precipitation in the model.

Figure 1 shows a map of the ADRIEX region with the regions of the aircraft measurements and nearby AERONET sites marked. The aircraft measurements are localized to three relatively small regions. The BAe 146 aircraft flew 43 science hours of which 9 hours were over the Po valley, 26 hours were over the Adriatic Sea and 8 hours were during the Black Sea flight. Further details of the aircraft aims and procedures are documented in Highwood *et al.* (2007). Note that the aircraft measurements represent observations with a higher spatial and temporal resolution than the model is able to reproduce. Further, some of the observations may not necessarily be representative of spatial scales that global models are able to reproduce; this is particularly known for the Ispra station. A 532 nm backscatter lidar was located at Nicelli airport (close to Venice) during ADRIEX and was used to retrieve vertical profiles of aerosol optical properties (such as extinction coefficient) on a time-scale of about 5 profiles per hour (Barnaba *et al.*, 2007).

3. Results

3.1. Chemical composition

In this section a comparison with measurements of the aerosol chemical composition during the campaign will be performed. These will consist of FAAM aircraft *in situ* measurements as well as surface observations. The aircraft measurements are mainly from a Quadrupole Aerosol Mass Spectrometer (Q-AMS) but also by filter analysis of bulk aerosol samples (Crosier *et al.*, 2007). The size cut-off of the AMS and the filter lines onboard the BAe 146 is not precisely known, although submicron particle losses are considered to be minimal due to the short sample lines used. Concerning the AMS, the instrument transmission is 100% for particles in the 40–700 nm vacuum aerodynamic diameter range (Crosier *et al.*, 2007). The mean of the AMS data from seven flights in the Venice region is presented in the results. Regarding the filter lines, previous comparison with ground-based measurements showed that the inlet passes about 35% of the sea-salt mode (Andreae *et al.*, 2000). The surface measurements are made within EMEP and we show only PM2.5 (particles with diameter less than 2.5 μm) results.

Figure 2 shows chemical composition from the aircraft measurements and the model. The aircraft measurements are an average over all the flights in the Adriatic region and the modelled data is averaged over the area covered by these flights, from the surface to an altitude of around 4 km (the top of the aerosol layer), limited to the daytime. The agreement between the aircraft observations and the model for sulphate, ammonium and nitrate is all within 25%, although best for sulphate (within 10%). The model tends to underestimate the concentrations for carbonaceous particles. The BC concentration is less than half of the measurements and the underestimation is

DOI: 10.1002/qj

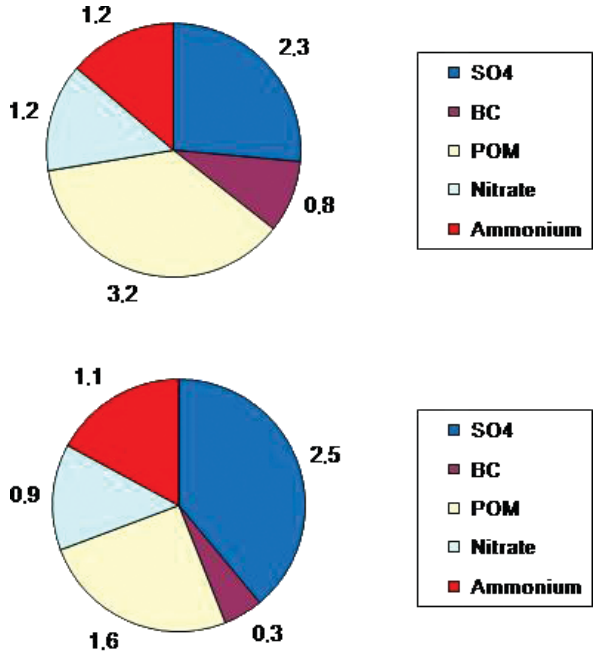

Figure 2. Aerosol chemical composition (g m^{-3}) during the ADRIEX campaign in 2004 for aircraft measurements (upper) and the aerosol model (lower). Aircraft measurements are the mean of collected data from the flights around the Venice area (Crosier *et al.*, 2007). The model results are from days with ADRIEX aircraft flights and sampled during daytime from land and sea areas around Venice.

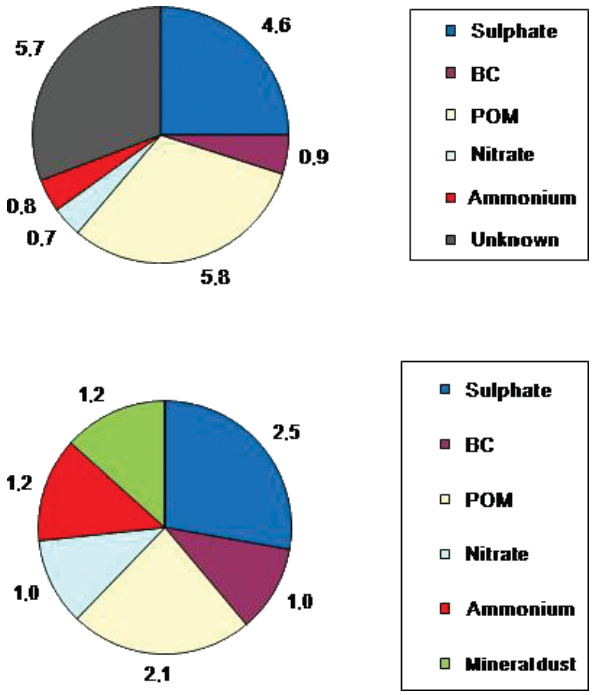

Figure 3. Aerosol chemical composition (g m^{-3}) from the EMEP station at Ispra (upper) and the model (lower) during the ADRIEX campaign.

large for the organic matter. However, the filter analysis during ADRIEX (Crosier *et al.*, 2007) showed a higher OC abundance than the AMS and indicated a rather low BC/OC ratio. BC/OC ratios from measurements and modelling are rather consistent (0.4 and 0.3, respectively). In Figure 2 the BC is from the filter analysis and the other components are from the AMS and thus the relative contribution from BC may not be completely consistent with the other components. In the model more than half of the organic matter is from secondary organic matter and the observations indicate that the main part of the organic matter is of secondary origin (Crosier *et al.*, 2007). The change in equilibrium constant compared to the standard version for ammonium nitrate leads to a 100% increase in the ammonium nitrate concentration. However, the nitrate is still somewhat underestimated in the model compared to the AMS. In the model, 80% of the nitrate is ammonium nitrate and the remaining fraction consists of nitrate on sea salt particles (only the fine mode of the sea salt particles is taken into account here). Also in the measurements a small fraction of the nitrate is found associated with typically coarse mode aerosols, but then with mineral dust (Crosier *et al.*, 2007). The model has 50% more nitrate over the land than over the sea in the model grid points near Venice, and the observations show also a large land–sea contrast in the nitrate concentration (Crosier *et al.*, 2007). For the other aerosol components the model has much smaller land–sea differences.

In Figure 3, observed (PM2.5) surface concentrations from Ispra are compared with modelled values, where both are daily means over the campaign period. The modelled data represents mass concentrations for particles of diameter below 2.5 μm (all the mass of fine mode particles and calculated fraction of sea salt and mineral that is less than 2.5 μm). Compared to the aircraft measurements there are some differences. The BC is in much better agreement with the measurements at the surface compared to the aircraft measurements, whereas for sulphate the model underestimates the concentration, and nitrate is somewhat overestimated in the model. For organic matter the model also underestimates the concentration at the surface, by more than a factor of two. The measured BC/OC ratio is consistent with the aircraft measurements, whereas the modelled ratio is significantly higher (∼0.7). Again a large fraction of the modelled organic matter is secondary (around 40%). The modelled total mass is about half of the surface observations, but a large fraction in the observations is of unknown composition. Dust (Al, Si, Fe, Ca) is measured on the filters from the aircraft measurements, dominates the coarse fraction and is likely a contributor to the unknown mass of fine mode particles as well. Unfortunately, we cannot apportion its relative contribution as the total mass by weighing is not determined. Close to 10% of the modelled nitrate is on sea salt particles with a diameter of less than 2.5 μm. All the chloride in the sea salt aerosols at Ispra is replaced by nitrate. The remaining sodium in the fine mode sea salt particles is negligible. The change in equilibrium constant compared to the standard version for ammonium nitrate leads to a 170% increase in the ammonium nitrate concentration. The total nitrate concentration also involves some fine mode nitrate associated with sea salt and the total nitrate is also more than doubled by the change in the equilibrium constant for ammonium nitrate.

DOI: 10.1002/qj

The daily variability in the aerosol composition is smaller for the carbonaceous particles than for inorganic particles in the observations and the model at Ispra. The standard deviations of daily mean data, divided by the mean, range from 22 to 36% in observations and 17 to 25% in the model for the carbonaceous particles. For inorganic aerosol constituents (sulphate, nitrate and ammonium) the numbers are from 51 to 78% and 45 to 68%, respectively for the observations and the model. The variability in the nitrate is particularly large both in the observations and the model. Although there is slightly less variability in the model than the observations, the main characteristics are reproduced by the model.

The comparison with observations of the chemical composition shows that in particular the OM concentration is underestimated in the aerosol model, and this underestimation can be more than 50%. In the observations the OM concentration dominated in the ADRIEX region on average; however, in the early to middle part of the experiment, ammonium nitrate was the dominant species towards the top of the boundary layer (Crosier *et al.*, 2007). The high amount of nitrate in the early to middle part of the campaign is likely due to the heavy rainfall in advance of the campaign (Highwood *et al.*, 2007), allowing the ammonia to react to ammonium nitrate until higher sulphate abundances were reached. For the other aerosol components the disagreement between the model and observations is smaller and more variable between the aircraft and the surface observations. Comparing a global aerosol model with horizontal resolution of 1×1 degree with measurements representing much finer spatial and temporal scales is difficult, and thus it is encouraging that model results are within around 20% of the observations (except OM).

3.2. Vertical profiles

An average of 6 deep aircraft profiles of aerosol extinction coefficient from the 6 available flights shown in Osborne *et al.* (2007) in the Adriatic region is shown in Figure 4 to compare with the mean lidar profile for ADRIEX. The aircraft profile includes two ranges of the variability in the two main parts of the aerosol plume. The mean lidar profile was calculated using lidar profiles averaged over the morning or afternoon period appropriate to the time of the aircraft profile during each flight. The error in the lidar extinction is typically 20–25%. The mean model result for the days with aircraft flights is also shown in Figure 4. Near the surface the lidar measurements show much higher extinction than the aircraft measurements and the model. This can be explained by highly localised pollution from Venice that did not readily advect out to sea (Osborne *et al.*, 2007) or to measurement uncertainties such as loss of ammonium nitrate through volatilisation at moderate sampling temperature (ten Brink *et al.*, 2000). Except for the lowest 500–600 metres and around 2 km, the lidar and aircraft measurements agree well. Differences can probably be reconciled by modification during advection and the fact that the aircraft profiles are heavily slanted and thereby can contain horizontal inhomogeneities in the aerosol. The variation shown by the aircraft measurements is significant and can explain some differences because the aircraft data are based on 6 profiles whilst the lidar data are based on numerous retrievals.

The aerosol model has a vertical profile that has much smaller variability than the observations. Below 2 km the vertical profile from the model follows the observed pattern with decreasing extinction in the lowest levels close to the surface and then increasing extinction up to around 2 km, although the gradient is weaker in the model than the observations. The modelled vertical profile is mostly between the lidar and aircraft measurements below 2 km. The highest extinction around 2 km in the aircraft observations are observed in the 3–4 of the flights in the first half of the campaign (Osborne *et al.*, 2007); under these conditions ammonium nitrate was the largest

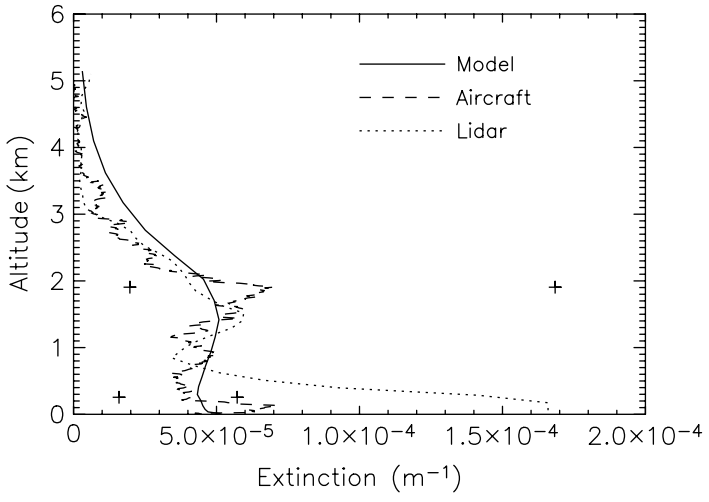

Figure 4. Aerosol vertical profile during ADRIEX from aircraft measurements, lidar, and the aerosol model. The aircraft measurements are a mean of vertical profiles taken during the campaign (Osborne *et al.*, 2007) and the aircraft data are averaged for each 10 m. The + represent the range in the aircraft data at two levels of the aerosol plume. The model results are from days with ADRIEX aircraft flights and sampled during daytime from land and sea areas around Venice.

DOI: 10.1002/qj

component of the fine mode aerosols (Crosier *et al.*, 2007) and likely to be a strong contributor to the high extinction around 2 km since nitrate has a rather high mass extinction. In the model, sulphate accounts for a large fraction of the extinction, and peaks around 1.5 km. Nitrate has a maximum around 2 km (in the region of maximum extinction in the aircraft measurements), where it accounts for slightly more than 25% of the extinction.

Although the extinction in the model in the upper part of the pollution layer is higher than the observations, the profile follows the pattern of the observations and the extinction is quite low at high altitude. Near the surface, carbonaceous aerosols contribute slightly less than half of the total extinction from the model, and an underestimation of these components could explain the lower extinction in the model near the surface. Above 2 km the extinction in the model is dominated by sulphate, but with significant contributions from nitrate and OM, e.g. between 3 and 4 km the extinction from nitrate and OM is very similar and the extinction from sulphate is close to the sum of these two components. Thus it is difficult to identify an aerosol component that is causing the overestimation above 2 km compared to the observations. It should also be noted that the variation in the vertical profile between the various flights is substantial (Osborne *et al.*, 2007) and that these profiles represent a spatial (probably also a temporal) scale that is not possible to cover in a global aerosol model with a horizontal resolution of 1×1 degree.

The vertical profile from Oslo CTM2 has also compared well with observations in two earlier campaigns, SAFARI-2000 and SHADE (Myhre *et al.*, 2003a; Myhre *et al.*, 2003b). This is important since the vertical profile of aerosols differs substantially between global aerosol models (Schwarz *et al.*, 2006; Textor *et al.*, 2006) and this is probably a major reason for the large difference in the radiative forcing of the direct aerosol effect (Schulz *et al.*, 2006).

3.3. Comparison between model and remote-sensed data from satellite and AERONET at AERONET stations

The global network of ground-based sunphotometers (AERONET) (Holben *et al.*, 1998) is used as a reference for aerosol optical depth (AOD) in validation of satellite retrievals and global aerosol modelling. Osborne *et al.* (2007) provided an analysis of AODs and fine mode-fractions from MODIS data (level 2 Collection 4 data) with AERONET and aircraft data during the ADRIEX campaign and find reasonable agreement. In the current investigation we compare updated Collection 5 AODs at 550 nm from the Moderate-resolution Imaging Spectrometer (MODIS: Remer *et al.*, 2005; Levy *et al.*, 2007) with the Multiangle Imaging Spectroradiometer (MISR: Kahn *et al.*, 2005), AERONET and with the model. The MODIS instrument is onboard the Terra and Aqua satellite platforms and thus both a morning and afternoon overpass are available. MISR is aboard the Terra platform with only a morning overpass. We use the MODIS Collection 5 dataset in the comparison of AOD. Several updates since the MODIS Collection 4 have been implemented into the over-land retrieval including a new surface reflectance treatment, the global aerosol optical models, and new calculations of the look-up tables (Levy *et al.*, 2007). The satellite data are shown for the level 3 products (1×1 degree resolution).

Figure 5 shows AOD from three AERONET stations in the Venice area (Highwood *et al.*, 2007) as well as from two Italian stations outside the operating area of the ADRIEX campaign region and one from the Black Sea area (where one aircraft flight took place as described in Cook *et al.* (2007)). The figure also shows AOD from the Oslo CTM2 (a standard simulation and one with a different set of emission data) and from two satellite retrievals. AERONET data and model results are daytime averages; whereas satellite data are instantaneous. The AERONET data in the Venice area show very low values at the beginning of the campaign period and increasing AOD values towards the middle of the period and thereafter somewhat lower values again (Highwood *et al.*, 2007). In advance of the ADRIEX campaign there was substantial rainfall and thus washout of the aerosols, explaining the low values at the beginning of the campaign. Further, the predominantly westerly wind swung to the east towards the end of the campaign (Highwood *et al.*, 2007). The aerosol model fails to reproduce the higher AOD values in the middle of the campaign period. The model does not calculate AOD values higher than 0.2 in the standard simulation at the three stations near Venice. As shown in subsection 3.1, the model underestimates the OM in the ADRIEX region. This is likely to explain most of the underestimation of AOD in the model, but there may also be a contribution from the high values of nitrate observed in the middle of the campaign which is somewhat underestimated in the model. In an additional simulation the primary OC and BC emission in the Po valley region have been increased by a factor of 10 and 5, respectively. The increased emission of primary carbonaceous aerosols enhance the AOD in the Venice area only slightly, and during the days with strongest underestimation compared to AERONET the difference compared to the standard calculation is negligible. This supports the conclusions from the observations that most of the OM is of secondary origin (Crosier *et al.*, 2007).

The MODIS satellite data compare well, with a few exceptions: an overestimation of the AOD during a few days (2 and 4 September 2004) and one day with an underestimation (1 September 2004) at the three stations near Venice. The few MISR data available in this region differ only slightly from the AERONET data. At Ispra the underestimation in the model is larger than at the Venice stations. For the MODIS data the agreement is good in the first part of the campaign, but there is a large overestimation of the AOD in the middle of the campaign period compared to the AERONET data at the Ispra site for the Terra data. At Lecce and Moldova the modelled AOD is in much better agreement with the AERONET data than at the stations in the Po valley

DOI: 10.1002/qj

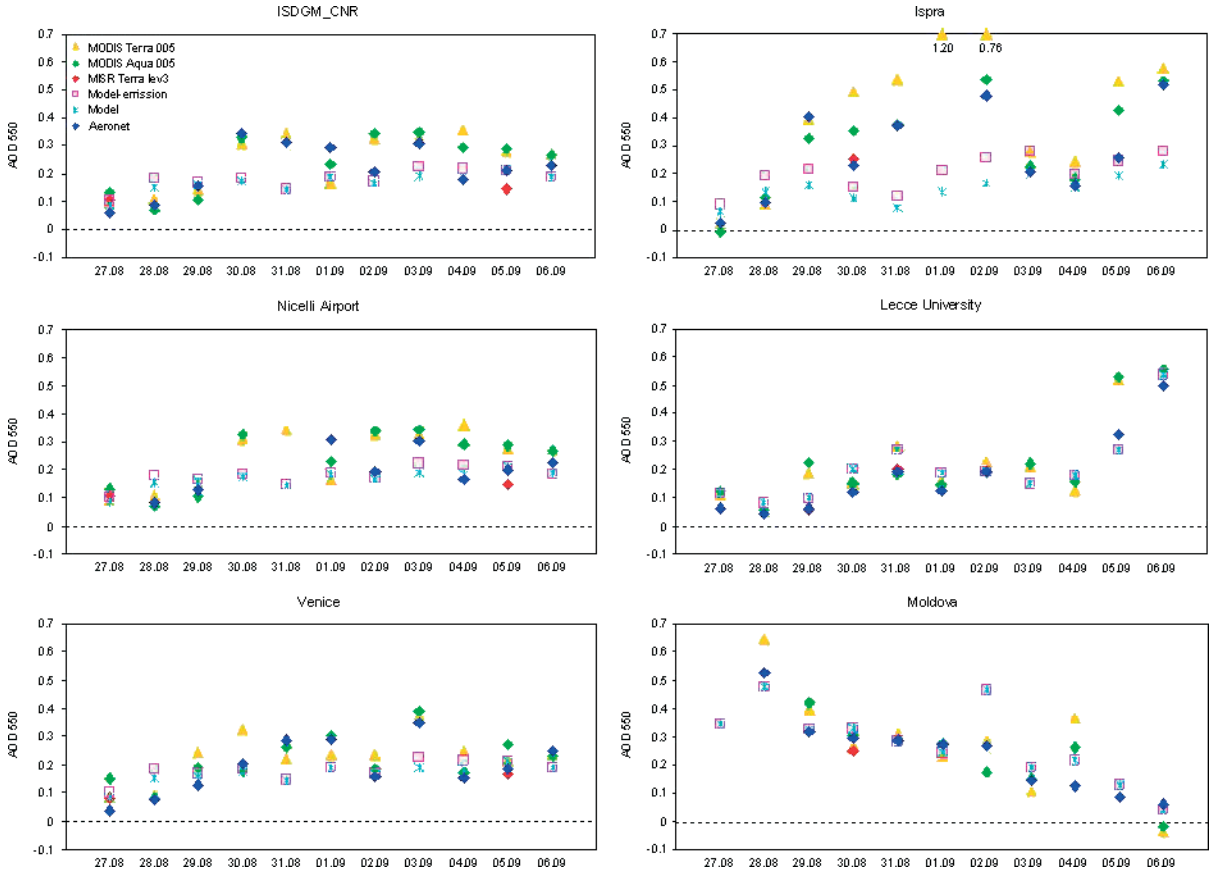

Figure 5. Aerosol optical depth (AOD) at 550 nm shown daily for AERONET, MODIS (onboard Terra and Aqua), MISR, and the aerosol model for 6 AERONET stations in the ADRIEX region. In addition to the standard aerosol model results (Model), results are shown for a simulation with increased primary carbonaceous emissions (Model-emission).

area. The model reproduces the variability as well as the level despite the large difference in AOD levels in Lecce and Moldova. At these two sites the chemical composition is more dominated by sulphate and partly by OM than at Venice and Ispra. Thus the better agreement can be explained by the better model performance for sulphate than other aerosol components. Further, the SOA abundance is generally higher in Oslo CTM2 in eastern Europe than in the Po valley region (Hoyle *et al.*, 2007). Observations also show a greater domination of sulphate in the Black Sea region compared to the Adriatic Sea (Crosier *et al.*, 2007). Also the agreement between AERONET and the satellite data is much better than in the Venice and Ispra stations.

The correlation between the model and the AERONET ranges from 0.41 in Ispra to 0.90 in Lecce, whereas near Venice the correlation ranges between 0.54 and 0.71. In Moldova the correlation is slightly lower than in Lecce. The recently released MODIS Collection 5 data (Levy *et al.*, 2007) shown in Figure 5 were compared with the older Collection 4 data. Even though the results of this comparison are not shown, the performance against the AERONET stations has significantly improved. The correlation coefficients are substantially higher in the Collection 5 data than in Collection 4, with smallest improvement at Ispra and largest improvement at Lecce. The Collection 5 MODIS data at Lecce now has correlation coefficients with the AERONET data of around 0.95.

At the six AERONET stations the MISR data compare very well, with a small tendency to lower values in the latter part of the experiment. The MODIS data differ especially at the three AERONET stations near Venice at the beginning of the period but also overestimate the AOD at other stations during the campaign. At Ispra an overestimation occurs over a period of a few days.

Except for 30 and 31 August for the three stations near Venice and 30 August and 2 September for Ispra, the AERONET daytime variation in AOD is rather small, and therefore diurnal variations cannot explain all of MODIS's differences from AERONET. MODIS and AERONET are each missing several days of data at various sites. For MODIS and partly for AERONET the missing data are associated with high cloud fractions (as derived from MODIS). However, the cloud fraction is rather small for the missing AERONET data at Nicelli Airport for the three days 27, 30 and 31 August, and AERONET level 1.0 and 1.5 are available there for those times.

3.4. Comparison of the spatial aerosol distributions obtained from model simulations and satellite retrievals

In Figure 6 the modelled AOD (550 nm) at 1200 UTC is compared to MODIS and MISR satellite-retrieved

DOI: 10.1002/qj

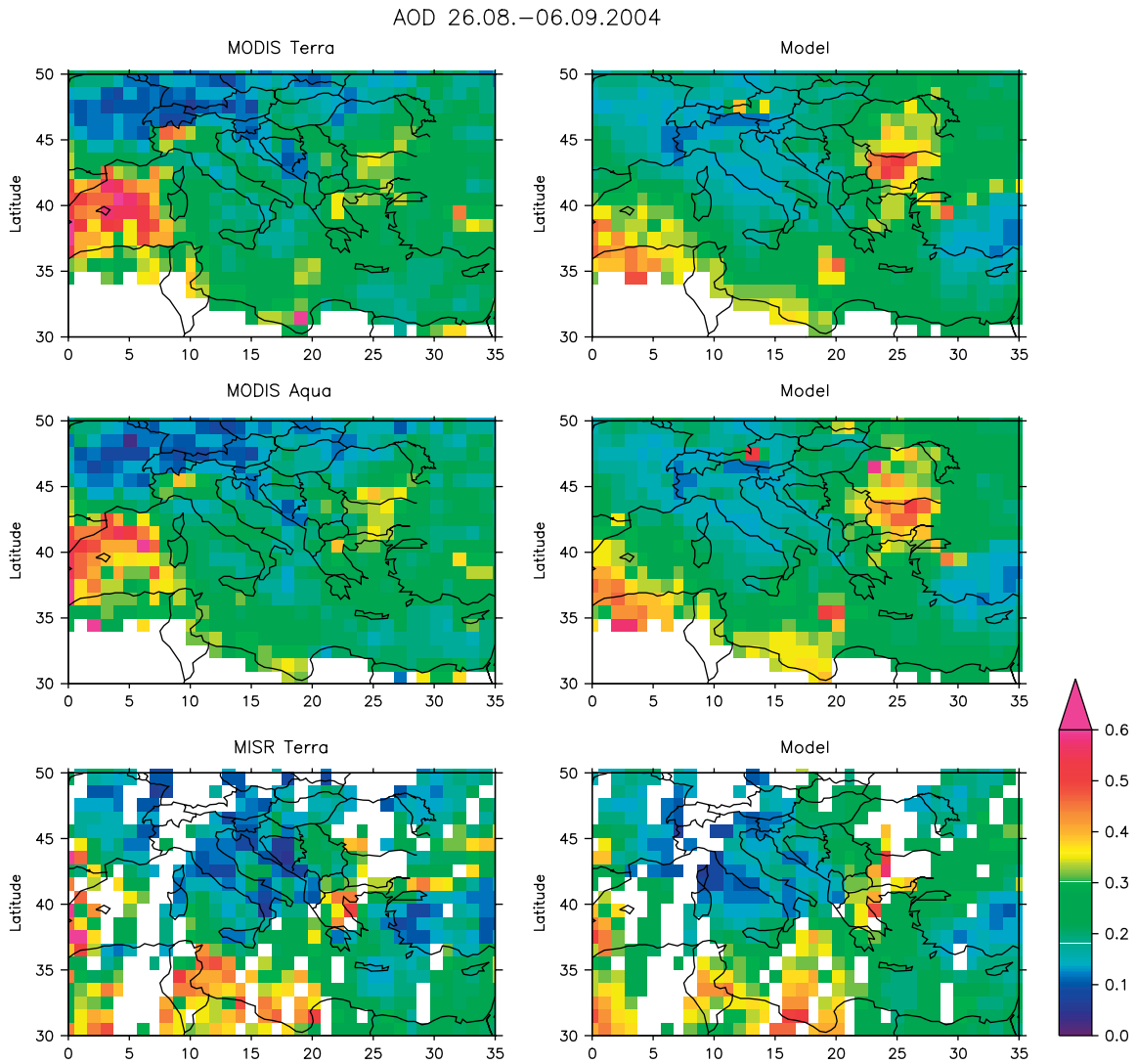

Figure 6. Mean AOD at 550 nm during the ADRIEX campaign for MODIS (onboard Terra and Aqua), MISR, and the aerosol model. For MODIS, Collection 4 and 5 data are shown. The results from the aerosol model have been screened to correspond to the daily satellite data, thus the model results shown in the right column vary.

AOD as a mean of available data during the campaign. The screening in the modelled data is performed so that grid boxes are only included if satellite data are available. Therefore the mean in the model shown in the right hand column of Figure 6 differs since it varies depending on which data are included. MODIS data for Collection 5 are shown in the figure. There is some small difference between the MODIS retrievals from Terra and Aqua. The dissimilarities between MODIS on Terra and Aqua are small compared to differences between MODIS and MISR. Part of this could be due to different screening of the data. The spatial coverage of the MISR data is lower than the MODIS data. MISR generally reports lower values, except that MISR retrieves more often in northern Africa where the surface reflectance is too high for standard MODIS retrievals. The pattern of the AOD distribution, high values in the western part of the Mediterranean and Spain as well as part of eastern Europe, is similar in the three satellite retrievals and the model. The Po valley region is a region where differences are evident between MODIS and MISR. The magnitude of the AOD between the various datasets is quite similar in the eastern part of Europe. Particularly high AOD values can be seen in south-east Europe, in outflow from the Sahara, and the Po valley (in MODIS), indicating large emissions of aerosol and their precursors in these regions. Over the Adriatic Sea, high AOD values are evident to the east and west (Po valley), but very low values to north and north-west, and the transported mineral dust from the Sahara seems not to reach this region significantly. The Mediterranean Sea has AOD values mostly above 0.2 in all the datasets shown in Figure 6. Overall the pattern in the modelled AOD is quite similar to MODIS Collection 5 and MISR with smaller AOD in the Po Valley and smaller mineral dust transported from Sahara in the model.

The mean of AOD from MISR over the region shown in Figure 6 is 0.23, equal to the model's value using screening necessary to match the MISR data. For MODIS

DOI: 10.1002/qj

Collection 5 the mean AOD is 0.21 and 0.20, respectively for MODIS on Terra and Aqua. The modelled mean AOD is 0.22 for a screening of the data similar to MODIS on Terra as well as for MODIS on Aqua. The spatial correlation coefficient between MISR and the model is 0.55, whereas for the model and MODIS on Terra and Aqua it ranges from 0.40 to 0.45.

3.5. Radiative forcing

For the radiative forcing of aerosols the single scattering albedo (SSA) is of crucial importance not only to estimate the magnitude of the forcing but even to estimate the sign (Haywood and Shine, 1995; Hansen *et al.*, 1997). A mean single scattering albedo of 0.92 at 550 nm is found in the aircraft measurements with quite some variability from 0.90 to 0.96 at 550 nm (Osborne *et al.*, 2007). In comparison the single scattering albedo in the Venice area is 0.93 in the model, ranging mostly from 0.90 to 0.95 at 550 nm. The mean of the three AERONET sites near Venice over the campaign period is 0.95 at 550 nm ranging from 0.88 to 0.98. For both the Ispra and Lecce AERONET stations the mean single scattering albedo is 0.93. The available single scattering albedo data from AERONET during the campaign are relatively sparse and are mainly in the latter part of the period. Even though the AOD from the model is lower than observations some days during ADRIEX, the aerosol optical properties are in close agreement with the observations (Osborne *et al.*, 2007).

Figure 7 shows direct radiative effect of aerosols (DRE) compared to satellite-derived estimate as well as normalized radiative effect (NRE) (direct radiative effect of aerosols divided by AOD at 550 nm) for the clear sky condition. The DREs from satellites are typically derived over the ocean and often includes both anthropogenic and natural aerosols. Three satellite-derived estimates are included in this analysis: (1) MODIS-R: The aerosol model used in the MODIS satellite retrieval is adopted to determine the aerosol optical properties and along with the AOD and an off-line radiative transfer model the DRE of aerosol is calculated (Remer and Kaufman, 2006). The MODIS-R data used in this study is based on the Collection 5 data. (2) MODIS-CERES-C: The MODIS aerosol product is combined with the Clouds and Earth Radiant Energy System (CERES) to derive the DRE (Christopher and Zhang, 2002; Zhang *et al.*, 2005). This method uses empirical aerosol angular dependence models derived from Terra (Zhang *et al.*, 2005). (3) MODIS-CERES-L: MODIS and CERES data combined to calculate the DRE of aerosols on a smaller spatial scale than for the CERES footprints (Loeb and Kato, 2002; Loeb and Manalo-Smith, 2005). Monthly mean data for August 2004 are used for the model and satellite-derived estimates in Figure 7, except for MODIS-CERES-L where monthly mean data for August 2001 are adopted. The data are based on diurnal mean values.

The modelled DRE varies between -6 and -8 W m^{-2} in the Adriatic Sea whereas values in the Black Sea are stronger. DRE in the southern part of the Mediterranean is mostly stronger than in the northern part which also follows the variation in AOD seen from Figure 6. The DRE of the aerosol over the Mediterranean Sea varies substantially between the various estimates in Figure 7 with differences in the northern part of the Adriatic Sea smaller than in the western Mediterranean and Black Sea and larger than in the south-eastern part of the Mediterranean. To avoid that difference in the AOD influences on the comparison of the aerosol radiative effect, we use the NRE as shown in Figure 7. Significant differences for the NRE of aerosols are found in the figure for the three satellite-derived products, and the model-derived NRE of aerosols is well within the range of the satellite data. The modelled NRE is quite similar in the Adriatic Sea and Black Sea with the former slightly stronger. Table I summarizes the DRE and NRE of aerosols in the northern part of the Adriatic Sea. The mean of the satellite-derived DRE of aerosols in the northern part of the Adriatic Sea is -8.4 W m^{-2} compared to the model -7.7 W m^{-2}. The mean of the NRE from the satellite estimates is -45.5 W m^{-2} in comparison to the model of -38.0 W m^{-2}. The table also shows that the variability in the DRE and NRE is relatively small over the northern part of the Adriatic Sea. Results are shown for August but are quite similar for September. The MODIS-R has a stronger DRE (and NRE) than the other estimates and uses an aerosol model in this region with a single scattering albedo of 0.96. In an additional model simulation it was shown that using this single scattering albedo gave only a cooling of 0.5 to 1.0 W m^{-2} stronger than for the modelled single scattering albedo, and thus the SSA cannot explain the difference in radiative effect.

The radiative forcing due to anthropogenic aerosols over Europe is shown in Figure 8 during the campaign period (all skies in the upper panel and clear skies in the lower panel). Natural aerosols such as mineral dust and sea salt are excluded in the simulations as well as pre-industrial levels of other aerosol types. Radiative forcing of magnitude of -2 to -5 W m^{-2} is simulated in the ADRIEX region. The radiative forcing is mostly weaker than this in the western part of Europe and stronger in parts of eastern Europe with values stronger than -10 W m^{-2} in certain parts of this area. Over the Mediterranean the difference between the clear and all sky is relative small due to the small cloud amount. With the measurements made during ADRIEX of vertical profiles of the aerosol and single scattering albedo in conjunction with the radiative forcing calculations, a positive radiative forcing can just about be ruled out during ADRIEX. An additional simulation with reduced modelled single scattering albedo of 0.03 resulted in negative radiative forcing only slightly weaker than shown in Figure 8 in the ADRIEX region.

DOI: 10.1002/qj

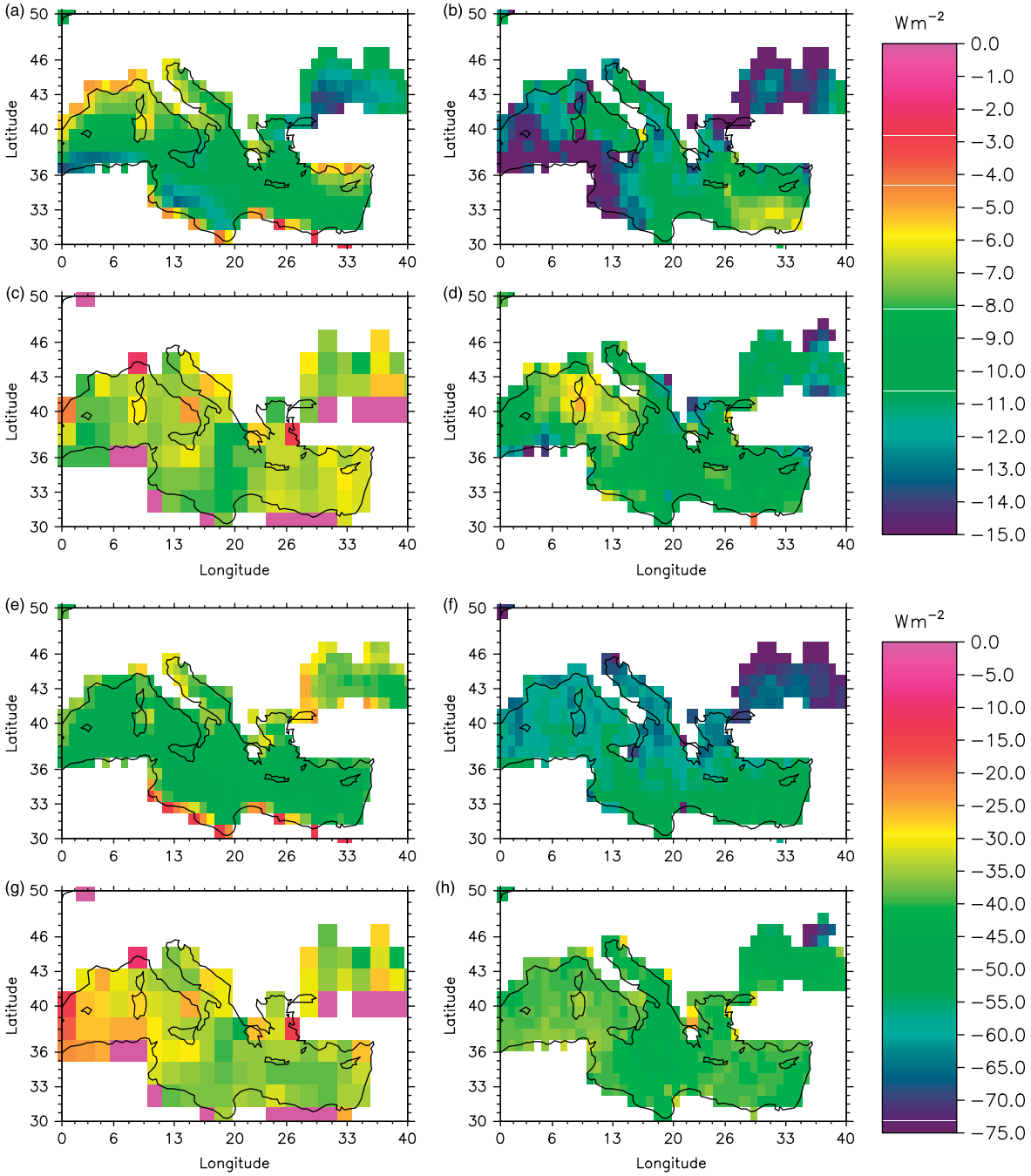

Figure 7. Direct radiative effect (DRE) and normalized radiative effect (DRE divided by AOD) (both given in W m^{-2}) over the sea for August 2004 for (a),(e) the model; (b),(f) MODIS-R; (c),(g) MODIS-CERES-C; (d),(h) MODIS-CERES-L (August 2001 data have been applied for the MODIS-CERES-L dataset). DRE (upper panel, (a)–(d)) and normalized radiative effect (lower panel, (e)–(h)).

4. Conclusion

The ADRIEX campaign took place in August and September 2004 in one of the European regions with moderate loadings of localized anthropogenic pollution and we report aerosol modelling in connection with this aerosol campaign. We have applied a global aerosol model with 1×1 degree resolution with all major aerosol components included. To improve the global aerosol models and the understanding of the climate effect of the aerosols it is vital to compare the models more with various aerosol observations. In this study we have compared the aerosol model with aircraft *in situ* observations of chemical composition, aerosol optical properties and aerosol vertical profiles, and to remote sensing from ground and satellites of AOD and the aerosol radiative effect.

The aerosol model reproduces the measurement results that most of the aerosols in the ADRIEX region are of secondary origin. However, the model underestimates the organic carbon amount in the ADRIEX region. The OC is certainly an important component in this region, and is mostly composed of SOA. The current understanding of physical and chemical processes associated with SOA is

DOI: 10.1002/qj

far from complete (Kanakidou *et al.*, 2005; Fuzzi *et al.*, 2006; Gelencsér *et al.*, 2007; Lukács *et al.*, 2007; Pio *et al.*, 2007; Robinson *et al.*, 2007). In this study we use a simulation where SOA is allowed to condense on sulphate aerosols in addition to primary OC aerosols and this forces the partitioning of the semi-volatile species more towards the aerosol phase, increasing the amount of SOA; however, even allowing all the SOA precursors to condense on existing aerosols is not sufficient to generate SOA amounts in accordance with the measurements (see the discussion in Hoyle *et al.* (2007)). This indicates that the underestimation in this region arises from a combination of insufficient knowledge of generation of SOA and emission of SOA precursors for this region. Particulate nitrate was also an important chemical constituent in the ADRIEX region with a significant land–sea difference. The model reproduces the observed significant land–sea difference with a strong gradient in the nitrate over the Adriatic Sea. Similar to observations of the vertical profile, the model results provide the largest role for nitrate at around 2 km. The spatial and temporal variation in the observed aerosol composition is substantial and, particularly for nitrate (Crosier *et al.*, 2007), the model reproduces the main pattern in

Table I. Radiative effects of aerosols from model and satellites

	Model	MODIS-R	MODIS-CERES-C	MODIS-CERES-L
Direct radiative effect	−7.7 (0.5)	−10.5 (0.4)	−6.2 (0.8)	−8.5 (0.8)
Normalized radiative effect	−38.0 (3.1)	−62.8 (3.4)	−32.8 (3.6)	−40.8 (0.9)

Direct radiative effect and normalized direct radiative effect (direct radiative effect divided by AOD) of aerosols from the aerosol model and three satellite-derived estimates over the northern part of the Adriatic Sea for August 2004. All values in W m^{-2}. Standard deviations are given in brackets.

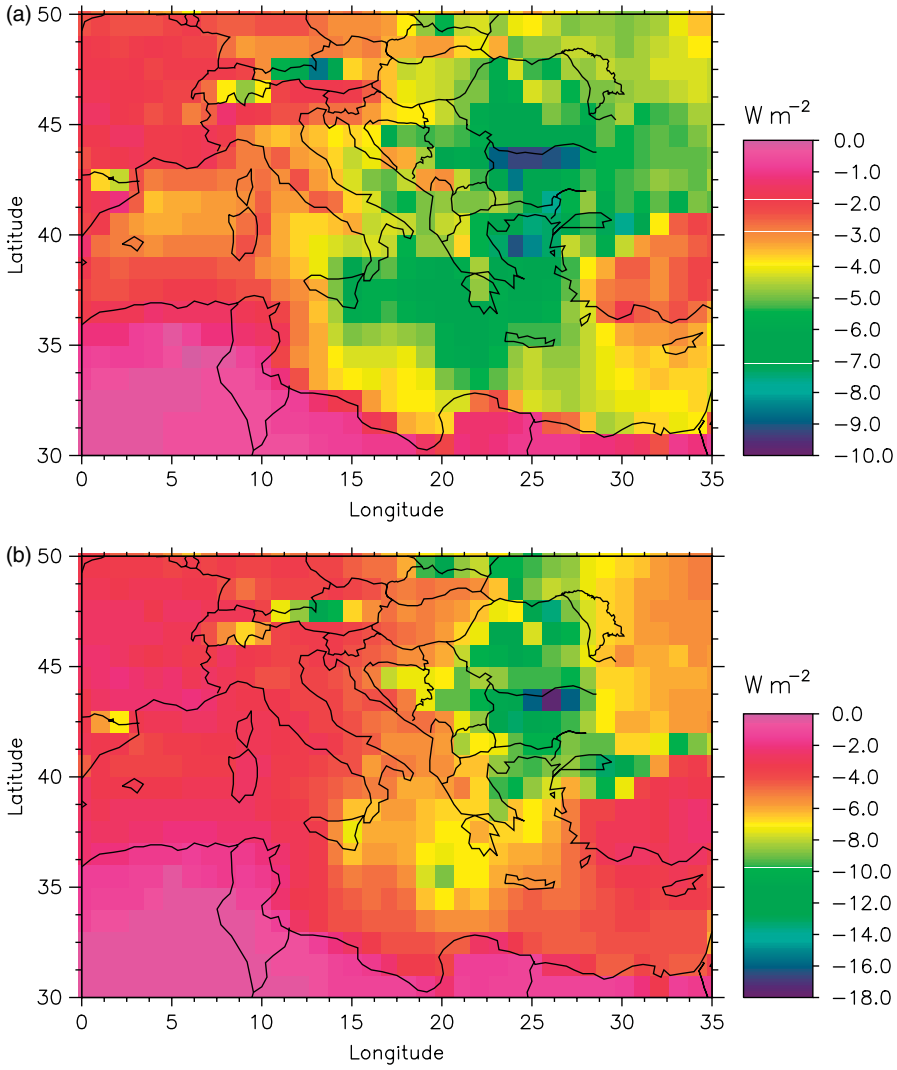

Figure 8. Radiative forcing (W m^{-2}) due to anthropogenic aerosols during ADRIEX for all sky conditions (upper) and clear sky condition (lower) simulated by the aerosol model.

DOI: 10.1002/qj

this variability, although with some underestimation of the nitrate abundance. We found also that the equilibrium constant was of crucial importance for calculating nitrate abundance in closer agreement with the measurements. We recommend the use of an equilibrium constant in the lower range of earlier recommendations as has been done in this study. Further investigations should be performed to quantify the equilibrium constant better.

The results illustrate clearly that the AOD at the most polluted site in this study region (Ispra) is underestimated in the model, but the model performs much better away from this region such as in Lecce and Moldova. In the Venice region the model underestimates the AOD somewhat compared to observations. Among the more than 100 AERONET stations for the year 2004, Ispra represents one of the AERONET station where the Oslo CTM aerosol model shows some of the largest underestimation (Myhre *et al.*, 2008) and is known to be a site where models have difficulty reproducing measurement results.

The single scattering albedo and the aerosol vertical profile are of crucial importance in estimating aerosol radiative forcing. For both of these parameters the model shows reasonable agreement with the observations. The modelled radiative effect of the aerosols (anthropogenic and natural) is within the range of satellite-derived estimates for the Mediterranean region (and the Adriatic Sea). However, the range between satellite-derived radiative effects is large. The source of this difference is unclear. A constant surface albedo in the MODIS-R retrieval may bias the DRE towards more negative values at high latitudes and may already influence the results for the Mediterranean Sea region. Also, conversion from instantaneous to daily mean DRE can be a reason for the differences.

We calculate a negative radiative forcing due to anthropogenic aerosols over the ADRIEX region (as well as the rest of Europe) in the period of the ADRIEX campaign in 2004. Based on the observations of chemical composition and of the single scattering albedo in combination with aerosol model simulations, we are treating this as a robust result for the ADRIEX region.

Acknowledgements

We appreciate the useful and constructive comments and suggestions from two reviewers. This study has received support from the Norwegian Research Council.

References

Andreae MO, Elbert W, Gabriel R, Johnson DW, Osborne S, Wood R. 2000. Soluble ion chemistry of the atmospheric aerosol and SO_2 concentrations over the eastern North Atlantic during ACE-2. *Tellus B* **52**: 1066–1087.

Ansari AS, Pandis SN. 1999. An analysis of four models predicting the partitioning of semivolatile inorganic aerosol components. *Aerosol Sci. Technol.* **31**: 129–153.

Barnaba F, Gobbi GP, de Leeuw G. 2007. Aerosol stratification, optical properties and radiative forcing in Venice (Italy) during ADRIEX. *Q. J. R. Meteorol. Soc.* **133**(S1): 47–60.

Bates TS, Huebert BJ, Gras JL, Griffiths FB, Durkee PA. 1998. International Global Atmospheric Chemistry (IGAC) project's first aerosol characterization experiment (ACE 1): Overview. *J. Geophys. Res.* **103**: 16297–16318.

Bellouin N, Boucher O, Haywood J, Reddy MS. 2005. Global estimate of aerosol direct radiative forcing from satellite measurements. *Nature* **438**: 1138–1141.

Berglen TF, Berntsen TK, Isaksen ISA, Sundet JK. 2004. A global model of the coupled sulfur/oxidant chemistry in the troposphere: The sulfur cycle. *J. Geophys. Res.* **109**: D19310, DOI:10.1029/2003JD003948.

Berntsen TK, Isaksen ISA. 1997. A global three-dimensional chemical transport model for the troposphere.1. Model description and CO and ozone results. *J. Geophys. Res.* **102**: 21239–21280.

Bond TC, Streets DG, Yarber KF, Nelson SM, Woo J-H, Klimont Z. 2004. A technology-based global inventory of black and organic carbon emissions from combustion. *J. Geophys. Res.* **109**: D14203, DOI: 10.1029/2003JD003697.

Bouwman AF, Lee DS, Asman WAH, Dentener FJ, van der Hoek KW, Olivier JGJ. 1997. A global high-resolution emission inventory for ammonia. *Global Biogeochem. Cycles* **11**: 561–587.

Christopher SA, Zhang J. 2002. Shortwave aerosol radiative forcing from MODIS and CERES observations over the oceans. *Geophys. Res. Lett.* **29**: 1859, DOI: 10.1029/2002GL014803.

Cook J, Highwood EJ, Coe H, Formenti P, Haywood JM, Crosier J. 2007. A comparison of aerosol optical and chemical properties over the Adriatic and Black Seas during summer 2004: Two case-studies from ADRIEX. *Q. J. R. Meteorol. Soc.* **133**(S1): 33–45.

Crosier J, Allan JD, Coe H, Bower KN, Formenti P, Williams PI. 2007. Chemical composition of summertime aerosol in the Po Valley (Italy), northern Adriatic and Black Sea. *Q. J. R. Meteorol. Soc.* **133**(S1): 61–75.

Dentener F, Kinne S, Bond T, Boucher O, Cofala J, Generoso S, Ginoux P, Gong S, Hoelzemann JJ, Ito A, Marelli L, Penner JE, Putaud J-P, Textor C, Schulz M, van der Werf GR, Wilson J. 2006. Emissions of primary aerosol and precursor gases in the years 2000 and 1750 prescribed data-sets for AeroCom. *Atmos. Chem. Phys.* **6**: 4321–4344.

Fuzzi S, Andreae MO, Huebert BJ, Kulmala M, Bond TC, Boy M, Doherty SJ, Guenther A, Kanakidou M, Kawamura K, Kerminen V-M, Lohmann U, Russell LM, Pöschl U. 2006. Critical assessment of the current state of scientific knowledge, terminology, and research needs concerning the role of organic aerosols in the atmosphere, climate, and global change. *Atmos. Chem. Phys.* **6**: 2017–2038.

Gelencsér A, May B, Simpson D, Sánchez-Ochoa A, Kasper-Giebl A, Puxbaum H, Caseiro A, Pio C, Legrand M. 2007. Source apportionment of PM2.5 organic aerosol over Europe: Primary/secondary, natural/anthropogenic, and fossil/biogenic origin. *J. Geophys. Res.* **112**: D23S04, DOI: 10.1029/2006JD008094.

Grini A, Myhre G, Sundet JK, Isaksen ISA. 2002. Modeling the annual cycle of sea salt in the global 3D model Oslo CTM2: Concentrations, fluxes, and radiative impact. *J. Climate* **15**: 1717–1730.

Grini A, Myhre G, Zender CS, Isaksen ISA. 2005. Model simulations of dust sources and transport in the global atmosphere: Effects of soil erodibility and wind speed variability. *J. Geophys. Res.* **110**: D02205, DOI: 10.1029/2004JD005037.

Hansen J, Sato M, Ruedy R. 1997. Radiative forcing and climate response. *J. Geophys. Res.* **102**: 6831–6864.

Haywood JM, Shine KP. 1995. The effect of anthropogenic sulfate and soot aerosol on the clear sky planetary radiation budget. *Geophys. Res. Lett.* **22**: 603–606.

Haywood JM, Francis P, Osborne S, Glew M, Loeb N, Highwood E, Tanré D, Myhre G, Formenti P, Hirst E. 2003. Radiative properties and direct radiative effect of Saharan dust measured by the C-130 aircraft during SHADE: 1. Solar spectrum. *J. Geophys. Res.* **108**: 8577, DOI: 10.1029/2002JD002687.

Highwood EJ, Haywood JM, Coe H, Cook J, Osborne S, Williams P, Crosier J, Bower K, Formenti P, McQuaid J, Brooks B, Thomas G, Grainger R, Barnaba F, Gobbi GP, de Leeuw G, Hopkins J. 2007. Aerosol Direct Radiative Impact Experiment (ADRIEX) overview. *Q. J. R. Meteorol. Soc.* **133**(S1): 3–15.

Holben BN, Eck TF, Slutsker I, Tanré D, Buis JP, Setzer A, Vermote E, Reagan JA, Kaufman YJ, Nakajima T, Lavenu F, Jankowiak I, Smirnov A. 1998. AERONET: A federated instrument network and data archive for aerosol characterization. *Remote Sensing Environ.* **66**: 1–16.

Hoyle CR, Berntsen T, Myhre G, Isaksen ISA. 2007. Secondary organic aerosol in the global aerosol – chemical transport model Oslo CTM2. *Atmos. Chem. Phys.* **7**: 5675–5694.

Kahn R, Anderson J, Anderson TL, Bates T, Brechtel F, Carrico CM, Clarke A, Doherty SJ, Dutton E, Flagan R, Frouin R, Fukushima H, Holben B, Howell S, Huebert B, Jefferson A, Jonsson H, Kalashnikova O, Kim J, Kim S-W, Kus P, Li W-H, Livingston JM, McNaughton C, Merrill J, Mukai S, Murayama T, Nakajima T, Quinn PK, Redemann J, Rood M, Russell P, Sano I, Schmid B, Seinfeld J, Sugimoto N, Wang J, Welton EJ, Won J-G, Yoon S-C. 2004. Environmental snapshots from ACE-Asia. *J. Geophys. Res.* **109**: D19S14, DOI: 10.1029/2003JD004339.

Kahn RA, Gaitley BJ, Martonchik JV, Diner DJ, Crean KA, Holben B. 2005. Multiangle Imaging Spectroradiometer (MISR) global aerosol optical depth validation based on 2 years of coincident Aerosol Robotic Network (AERONET) observations. *J. Geophys. Res.* **110**: D10S04, DOI: 10.1029/2004JD004706.

Kanakidou M, Seinfeld JH, Pandis SN, Barnes I, Dentener FJ, Facchini MC, van Dingenen R, Ervens B, Nenes A, Nielsen CJ, Swietlicki E, Putaud J-P, Balkanski Y, Fuzzi S, Horth J, Moortgat GK, Winterhalter R, Myhre CEL, Tsigaridis K, Vignati E, Stephanou EG, Wilson J. 2005. Organic aerosol and global climate modelling: A review. *Atmos. Chem. Phys.* **5**: 1053–1123.

Kaufman YJ, Tanré D, Boucher O. 2002. A satellite view of aerosols in the climate system. *Nature* **419**: 215–223.

Kinne S, Schulz M, Textor C, Guibert S, Balkanski Y, Bauer SE, Berntsen T, Berglen TF, Boucher O, Chin M, Collins W, Dentener F, Diehl T, Easter R, Feichter J, Fillmore D, Ghan S, Ginoux P, Gong S, Grini A, Hendricks JE, Herzog M, Horowitz L, Isaksen L, Iversen T, Kirkevåg A, Kloster S, Koch D, Kristjansson JE, Krol M, Lauer A, Lamarque JF, Lesins G, Liu X, Lohmann U, Montanaro V, Myhre G, Penner JE, Pitari G, Reddy S, Seland O, Stier P, Takemura T, Tie X. 2006. An AeroCom initial assessment – optical properties in aerosol component modules of global models. *Atmos. Chem. Phys.* **6**: 1815–1834.

Lelieveld J, Crutzen PJ, Ramanathan V, Andreae MO, Brenninkmeijer CAM, Campos T, Cass GR, Dickerson RR, Fischer H, de Gouw JA, Hansel A, Jefferson A, Kley D, de Laat ATJ, Lal S, Lawrence MG, Lobert JM, Mayol-Bracero OL, Mitra AP, Novakov T, Oltmans SJ, Prather KA, Reiner T, Rodhe H, Scheeren HA, Sikka D, Williams J. 2001. The Indian Ocean Experiment: Widespread air pollution from south and southeast Asia. *Science* **291**: 1031–1036.

Lelieveld J, Berresheim H, Borrmann S, Crutzen PJ, Dentener FJ, Fischer H, Feichter J, Flatau PJ, Heland J, Holzinger R, Korrmann R, Lawrence MG, Levin Z, Markowicz KM, Mihalopoulos N, Minikin A, Ramanathan V, de Reus M, Roelofs GJ, Scheeren HA, Sciare J, Schlager H, Schultz M, Siegmund P, Steil B, Stephanou EG, Stier P, Traub M, Warneke C, Williams J, Ziereis H. 2002. Global air pollution crossroads over the Mediterranean. *Science* **298**: 794–799.

Levy RC, Remer LA, Mattoo S, Vermote EF, Kaufman YJ. 2007. Second-generation operational algorithm: Retrieval of aerosol properties over land from inversion of Moderate Resolution Imaging Spectroradiometer spectral reflectance. *J. Geophys. Res.* **112**: D13211, DOI: 10.1029/2006JD007811.

Loeb NG, Kato S. 2002. Top-of-atmosphere direct radiative effect of aerosols over the tropical oceans from the Clouds and the Earth's Radiant Energy System (CERES) satellite instrument. *J. Climate* **15**: 1474–1484.

Loeb NG, Manalo-Smith N. 2005. Top-of-atmosphere direct radiative effect of aerosols over global oceans from merged CERES and MODIS observations. *J. Climate* **18**: 3506–3526.

Lukács H, Gelencsér A, Hammer S, Puxbaum H, Pio C, Legrand M, Kasper-Giebl A, Handler M, Limbeck A, Simpson D, Preunkert S. 2007. Seasonal trends and possible sources of brown carbon based on 2-year aerosol measurements at six sites in Europe. *J. Geophys. Res.* **112**: D23S18, DOI: 10.1029/2006JD008151.

Maria SF, Russell LM, Gilles MK, Myneni SCB. 2004. Organic aerosol growth mechanisms and their climate-forcing implications. *Science* **306**: 1921–1924.

Metzger S, Dentener F, Pandis S, Lelieveld J. 2002a. Gas/aerosol partitioning. 1. A computationally efficient model. *J. Geophys. Res.* **107**: 4312, DOI: 10.1029/2001JD001102.

Metzger S, Dentener F, Krol M, Jeuken A, Lelieveld J. 2002b. Gas/aerosol partitioning. 2. Global modeling results. *J. Geophys. Res.* **107**: 4313, DOI:10.1029/2001JD001103.

Myhre G, Berntsen TK, Haywood JM, Sundet JK, Holben BN, Johnsrud M, Stordal F. 2003a. Modeling the solar radiative impact of aerosols from biomass burning during the Southern African Regional Science Initiative (SAFARI-2000) experiment. *J. Geophys. Res.* **108**: 8501, DOI: 10.1029/2002JD002313.

Myhre G, Grini A, Haywood JM, Stordal F, Chatenet B, Tanré D, Sundet JK, Isaksen ISA. 2003b. Modeling the radiative impact of mineral dust during the Saharan Dust Experiment (SHADE) campaign. *J. Geophys. Res.* **108**: 8579, DOI: 10.1029/2002JD002566.

Myhre G, Stordal F, Berglen TF, Sundet JK, Isaksen ISA. 2004. Uncertainties in the radiative forcing due to sulfate aerosols. *J. Atmos. Sci.* **61**: 485–498.

Myhre G, Grini A, Metzger S. 2006. Modelling of nitrate and ammonium-containing aerosols in presence of sea salt. *Atmos. Chem. Phys.* **6**: 4809–4821.

Myhre G, Bellouin N, Berglen TF, Berntsen TK, Boucher O, Grini A, Isaksen ISA, Johnsrud M, Mishchenko MI, Stordal F, Tanré D. 2007. Comparison of the radiative properties and direct radiative effect of aerosols from a global aerosol model and remote sensing data over ocean. *Tellus B* **59**: 115–129.

Myhre G, Berglen TF, Johnsrud M, Hoyle CR, Berntsen TK, Christopher SA, Fahey DW, Isaksen ISA, Jones TA, Kahn RA, Loeb N, Quinn PK, Remer L, Schwartz JP, Yttri KE. 2008. Radiative forcing of the direct aerosol effect using a multi-observation approach. *Atmos. Chem. Phys. Discuss.* **8**: 12823–12886.

Novakov T, Hegg DA, Hobbs PV. 1997. Airborne measurements of carbonaceous aerosols on the East Coast of the United States. *J. Geophys. Res.* **102**: 30023–30030.

Odum JR, Hoffmann T, Bowman F, Collins D, Flagan RC, Seinfeld JH. 1996. Gas/particle partitioning and secondary organic aerosol yields. *Environ. Sci. Technol.* **30**: 2580–2585.

Olivier J, Peters J, Granier C, Petron G, Muller JF, Wallens S. 2003. Present and future surface emissions of atmospheric compounds. POET Report No. 2, EU project EVK2-1999-00011.

Osborne SR, Haywood JM, Bellouin N. 2007. *In situ* and remote-sensing measurements of the mean microphysical and optical properties of industrial pollution aerosol during ADRIEX. *Q. J. R. Meteorol. Soc.* **133**(S1): 17–32.

Pio CA, Legrand M, Oliveira T, Afonso J, Santos C, Caseiro A, Fialho P, Barata F, Puxbaum H, Sanchez-Ochoa A, Kasper-Giebl A, Gelencsér A, Preunkert S, Schock M. 2007. Climatology of aerosol composition (organic versus inorganic) at nonurban sites on a west–east transect across Europe. *J. Geophys. Res.* **112**: D23S02, DOI: 10.1029/2006JD008038.

Polidori A, Turpin BJ, Davidson CI, Rodenburg LA, Maimone F. 2008. Organic PM2.5: Fractionation by polarity, FTIR spectroscopy, and OM/OC ratio for the Pittsburgh aerosol. *Aerosol Sci. Technol.* **42**: 233–246.

Putaud J-P, Raes F, van Dingenen R, Brüggemann E, Facchini M-C, Decesari S, Fuzzi S, Gehrig R, Hüglin C, Laj P, Lorbeer G, Maenhaut W, Mihalopoulos N, Müller K, Querol X, Rodriguez S, Schneider J, Spindler G, ten Brink H, Tørseth K, Wiedensohler A. 2004. A European aerosol phenomenology. 2: Chemical characteristics of particulate matter at kerbside, urban, rural and background sites in Europe. *Atmos. Environ.* **38**: 2579–2595.

Quinn PK, Bates TS. 2005. Regional aerosol properties: Comparisons of boundary layer measurements from ACE 1, ACE 2, Aerosols99, INDOEX, ACE Asia, TARFOX, and NEAQS. *J. Geophys. Res.* **110**: D14202, DOI: 10.1029/2004JD004755.

Raes F, Bates T, McGovern F, van Liedekerke M. 2000. The 2nd Aerosol Characterization Experiment (ACE-2): General overview and main results. *Tellus B* **52**: 111–125.

Ramanathan V, Crutzen PJ, Lelieveld J, Mitra AP, Althausen D, Anderson J, Andreae MO, Cantrell W, Cass GR, Chung CE, Clarke AD, Coakley JA, Collins WD, Conant WC, Dulac F, Heintzenberg J, Heymsfield AJ, Holben B, Howell S, Hudson J, Jayaraman A, Kiehl JT, Krishnamurti TN, Lubin D, McFarquhar G, Novakov T, Ogren JA, Podgorny IA, Prather K, Priestley K, Prospero JM, Quinn PK, Rajeev K, Rasch P, Rupert S, Sadourny R, Satheesh SK, Shaw GE, Sheridan P, Valero FPJ. 2001. Indian Ocean Experiment: An integrated analysis of the climate forcing and effects of the great Indo-Asian haze. *J. Geophys. Res.* **106**: 28371–28398.

Remer LA, Kaufman YJ. 2006. Aerosol direct radiative effect at the top of the atmosphere over cloud free ocean derived from four years of MODIS data. *Atmos. Chem. Phys.* **6**: 237–253.

Remer LA, Kaufman YJ, Tanré D, Mattoo S, Chu DA, Martins JV, Li R-R, Ichoku C, Levy RC, Kleidman RG, Eck TF, Vermote E, Holben BN. 2005. The MODIS aerosol algorithm, products, and validation. *J. Atmos. Sci.* **62**: 947–973.

Robinson AL, Donahue NM, Shrivastava MK, Weitkamp EA, Sage AM, Grieshop AP, Lane TE, Pierce JR, Pandis SN. 2007. Rethinking organic aerosols: Semivolatile emissions and photochemical aging. *Science* **315**: 1259–1262.

Satheesh SK, Ramanathan V. 2000. Large differences in tropical aerosol forcing at the top of the atmosphere and Earth's surface. *Nature* **405**: 60–63.

Schulz M, Textor C, Kinne S, Balkanski Y, Bauer S, Berntsen T, Berglen T, Boucher O, Dentener F, Guibert S, Isaksen ISA, Iversen T, Koch D, Kirkevåg A, Liu X, Montanaro V, Myhre G, Penner JE, Pitari G, Reddy S, Seland Ø, Stier P, Takemura T. 2006. Radiative forcing by aerosols as derived from the AeroCom present-day and pre-industrial simulations. *Atmos. Chem. Phys.* **6**: 5225–5246.

Schwarz JP, Gao RS, Fahey DW, Thomson DS, Watts LA, Wilson JC, Reeves JM, Darbeheshti M, Baumgardner DG, Kok GL, Chung SH, Schulz M, Hendricks J, Lauer A, Kärcher B, Slowik JG, Rosenlof KH, Thompson TL, Langford AO, Loewenstein M, Aikin KC. 2006. Single-particle measurements of midlatitude black carbon and light-scattering aerosols from the boundary layer to the lower stratosphere. *J. Geophys. Res.* **111**: D16207, DOI: 10.1029/2006JD007076.

Swap RJ, Annegarn HJ, Suttles JT, King MD, Platnick S, Privette JL, Scholes RJ. 2003. Africa burning: A thematic analysis of the Southern African Regional Science Initiative (SAFARI 2000). *J. Geophys. Res.* **108**: 8465, DOI: 10.1029/2003JD003747.

Tanré D, Haywood J, Pelon J, Léon JF, Chatenet B, Formenti P, Francis P, Goloub P, Highwood EJ, Myhre G. 2003. Measurement and modeling of the Saharan dust radiative impact: Overview of the Saharan Dust Experiment (SHADE). *J. Geophys. Res.* **108**: 8574, DOI: 10.1029/2002JD003273.

ten Brink HM, Khlystov A, Kos GPA, Tuch T, Roth C, Kreyling W. 2000. A high-flow humidograph for testing the water uptake by ambient aerosol. *Atmos. Environ.* **34**: 4291–4300.

Textor C, Schulz M, Guibert S, Kinne S, Balkanski Y, Bauer S, Berntsen T, Berglen T, Boucher O, Chin M, Dentener F, Diehl T, Easter R, Feichter H, Fillmore D, Ghan S, Ginoux P, Gong S, Grini A, Hendricks J, Horowitz L, Huang P, Isaksen ISA, Iversen T, Kloster S, Koch D, Kirkevåg A, Kristjansson JE, Krol M, Lauer A, Lamarque JF, Liu X, Montanaro V, Myhre G, Penner J, Pitari G, Reddy S, Seland Ø, Stier P, Takemura T, Tie X. 2006. Analysis and quantification of the diversities of aerosol life cycles within AeroCom. *Atmos. Chem. Phys.* **6**: 1777–1813.

Turpin BJ, Lim H-J. 2001. Species contributions to PM2.5 mass concentrations: Revisiting common assumptions for estimating organic mass. *Aerosol Sci. Technol.* **35**: 602–610.

van der Werf GR, Randerson JT, Giglio L, Collatz GJ, Kasibhatla PS, Arellano Jr AF. 2006. Interannual variability in global biomass burning emissions from 1997 to 2004. *Atmos. Chem. Phys.* **6**: 3423–3441.

Vestreng V, Myhre G, Fagerli H, Reis S, Tarrasón L. 2007. Twenty-five years of continuous sulphur dioxide emission reduction in Europe. *Atmos. Chem. Phys.* **7**: 3663–3681.

Zhang J, Christopher SA, Remer LA, Kaufman YJ. 2005. Shortwave aerosol radiative forcing over cloud-free oceans from Terra: 1. Angular models for aerosols. *J. Geophys. Res.* **110**: D10S23, DOI: 10.1029/2004JD005008.